

Striatal Astrocytes Transdifferentiate into Functional Mature Neurons Following Ischemic Brain Injury

Chun-Ling Duan,^{1,2} Chong-Wei Liu,^{1,2} Shu-Wen Shen,^{1,2} Zhang Yu,³ Jia-Lin Mo,^{1,2,4}
Xian-Hua Chen,^{1,2} and Feng-Yan Sun^{1,2,4}

To determine whether reactive astrocytes stimulated by brain injury can transdifferentiate into functional new neurons, we labeled these cells by injecting a glial fibrillary acidic protein (GFAP) targeted enhanced green fluorescence protein plasmid (pGfa2-eGFP plasmid) into the striatum of adult rats immediately following a transient middle cerebral artery occlusion (MCAO) and performed immunolabeling with specific neuronal markers to trace the neural fates of eGFP-expressing (GFP⁺) reactive astrocytes. The results showed that a portion of striatal GFP⁺ astrocytes could transdifferentiate into immature neurons at 1 week after MCAO and mature neurons at 2 weeks as determined by double staining GFP-expressing cells with β III-tubulin (GFP⁺-Tuj-1⁺) and microtubule associated protein-2 (GFP⁺-MAP-2⁺), respectively. GFP⁺ neurons further expressed choline acetyltransferase, glutamic acid decarboxylase, dopamine receptor D2-like family proteins, and the N-methyl-D-aspartate receptor subunit R2, indicating that astrocyte-derived neurons could develop into cholinergic or GABAergic neurons and express dopamine and glutamate receptors on their membranes. Electron microscopy analysis indicated that GFP⁺ neurons could form synapses with other neurons at 13 weeks after MCAO. Electrophysiological recordings revealed that action potentials and active postsynaptic currents could be recorded in the neuron-like GFP⁺ cells but not in the astrocyte-like GFP⁺ cells, demonstrating that new GFP⁺ neurons possessed the capacity to fire action potentials and receive synaptic inputs. These results demonstrated that striatal astrocyte-derived new neurons participate in the rebuilding of functional neural networks, a fundamental basis for brain repair after injury. These results may lead to new therapeutic strategies for enhancing brain repair after ischemic stroke.

GLIA 2015;63:1660–1670

Key words: neural network, glia, neurogenesis, stem cell, brain repair

Introduction

Stroke activates endogenous neural repair in response to neuronal damage caused by various signaling pathways (Graham and Chen, 2001; Lipton, 1999) to avoid further brain damage (Dirnagl et al., 2003). Theoretically, improving this endogenous protective/repair capacity could be a valuable therapeutic approach for stroke treatment. Ischemic stroke induced neurogenesis (Arvidsson et al., 2002), an endogenous form of neural repair, has shown that newly generated neurons migrate to the damaged brain region (Arvidsson et al.,

2002; Li et al., 2010; Wang et al., 2007; Yamashita et al., 2006) and integrate into local (Hou et al., 2008) and distal neural networks (Guo et al., 2012; Sun et al., 2012; Zhang et al., 2013) in the non-neurogenic regions. These findings indicate that newly generated neurons play important roles in the morphological and functional reconstructive repair of the brain after injury. The origin of new neurons in the striatum, one of the most damaged non-neurogenic regions following middle cerebral artery occlusion (MCAO), is still debated, although at least a portion of neurons migrate from the

View this article online at wileyonlinelibrary.com. DOI: 10.1002/glia.22837

Published online June 1, 2015 in Wiley Online Library (wileyonlinelibrary.com). Received Nov 26, 2014, Accepted for publication Mar 29, 2015.

Address correspondence to Feng-Yan Sun, Department of Neurobiology, Shanghai Medical College of Fudan University, 138, Yi-Xue-Yuan Road, Shanghai 200032, P. R. China. E-mail: fysun@shmu.edu.cn

¹From the Department of Neurobiology, School of Basic Medical Science, Shanghai Medical College, Fudan University, Shanghai, People's Republic of China;

²Research Unit of Brain Injury, State Key Laboratory of Medical Neurobiology, Shanghai Medical College, Fudan University, Shanghai, People's Republic of China;

³The Electron Microscopy Core Laboratory, School of Basic Medical Science, Shanghai Medical College, Fudan University, Shanghai, People's Republic of China;

⁴Research Institute of Aging Biology, Research Center on Aging and Medicine and Institutes for Biomedical Science, Shanghai Medical College, Fudan University, Shanghai, People's Republic of China

Chun-Ling Duan and Chong-Wei Liu contributed equally to this work.

subventricular zone (SVZ), a major neurogenic region (Arvidsson et al., 2002).

It has been demonstrated that GFAP-expressing astroglia in the SVZ act as neural stem cells in adult mammalian brains (Alvarez-Buylla et al., 2000). Mature astrocytes in non-neurogenic regions can be reactivated and proliferated in response to cerebral ischemic stroke or traumatic injury, which is characterized by the increased expression of GFAP (Liu et al., 2002; Pekny and Nilsson, 2005) and re-expression of nestin/vimentin (Buffo et al., 2008; Liu et al., 2002; Liu et al., 2003), which is referred to as astrogliosis. *In vitro* and *in vivo* studies have demonstrated the transdifferentiation potential of astrocytes. For example, cultured astroglial cells from the early postnatal cerebral cortex can be directed toward a neuronal lineage by overexpressing neurogenin-2 (Ngn2) or mammalian achaete-scute homolog 1 (Mash1) (Berninger et al., 2007). Interestingly, Dr. Zhang's laboratory found that a single transcription factor, Sox2, was sufficient to reprogram resident astrocytes into proliferative neuroblasts in the intact brain of adult mice (Niu et al., 2013). Additionally, Kronenberg et al. reported that resident Pax6-expressing astrocytes developed a neurogenic potential (Kronenberg et al., 2010). More interestingly, recent findings have indicated that cerebral middle artery ischemic stroke causes striatal neurogenesis in endogenous astrocytes, which could be upregulated by inhibition of notch-1 signaling (Qin et al., 2014). However, it is still unknown whether resident reactive astrocytes in non-neurogenic regions of adult ischemically injured brains can transdifferentiate into functional mature neurons, which is of fundamental clinical importance for brain repair after damage.

In this study, we successfully labeled local reactive astrocytes by injecting pGfa2-eGFP plasmids driven by human GFAP promoter into the ipsilateral striatum of adult rats immediately following a transient MCAO. We combined GFP-labeling with immunostaining for neuronal lineage markers to determine whether ischemia could cause GFP⁺ reactive astrocytes to transdifferentiate into neurons. Electron microscopy and electrophysiological recordings were used to study the synaptic formation and functional synaptic transmission of astrocyte-derived neurons. We found that subsets of striatal astrocytes were capable of transdifferentiating into new mature neurons and functionally integrating into neuronal networks. These results provide important evidence that striatal reactive astrocytes are a subpopulation of endogenous neural precursors for post-stroke neurogenesis and thus play a beneficial role in neuronal repair after injury.

Materials and Methods

Animals

Male Sprague-Dawley rats (220–250 g) from the Shanghai Experimental Animal Center of the Chinese Academy of Sciences were

used for this study. This study was conducted in accordance with the National Institutes of Health Guide for the Care and Use of Laboratory Animals, and the protocols were approved by the Medical Experimental Animal Administrative Committee of Shanghai Medical College of Fudan University. All efforts were made to minimize animal suffering and reduce the number of animals used.

Transient Middle Cerebral Artery Occlusion (MCAO)

Rats were anesthetized with 10% chloral hydrate (360 mg/kg, i.p.). Arterial blood samples obtained via a femoral catheter were collected to measure the pO₂, pCO₂, and pH using an AVL 990 Blood Gas Analyzer (AVL List GmbH, Graz, Austria). The rectal temperature was maintained at 37 ± 0.5°C via a temperature-regulated heating lamp (Wang et al., 2007). Rats with physiological variables within normal ranges were subjected to transient focal cerebral ischemia induced by a left MCAO as described previously (Longa et al., 1989; Zhang et al., 2006). In brief, a 4-0 nylon monofilament with a rounded tip was introduced into the left external carotid artery lumen and gently advanced into the internal carotid artery until slight resistance was felt. The filament was left in place for 30 min and then withdrawn.

Administration of 5'-Bromodeoxyuridine (BrdU)

To detect whether reactive astrocytes were dividing, rats were intraperitoneally injected with freshly prepared BrdU (50 mg/kg body weight; Roche, Mannheim, Germany) 3 days after a MCAO and sacrificed 2 h later.

Administration of pGfa2-eGFP Plasmids

The pGfa2-eGFP plasmid, which expressed the enhanced green fluorescent protein (eGFP) reporter gene driven by a 2.2 kb human GFAP promoter, was kindly provided by Dr. Michael Brenner through the Alabama Neuroscience Blueprint Core (NIH grants NS39055 and NS057098) (Nolte et al., 2001; Su et al., 2004). Within 15 min of reperfusion after a MCAO, stereotaxic injection of the plasmid was performed in deeply anesthetized rats placed in a stereotaxic frame (Narishige, Tokyo, Japan). A 3 µL volume of the plasmid mixture (1 µL of 5 µg/µL plasmids, 1 µL of sterile saline, and 1 µL of Lipofectamine 2000 at 1:1:1 volume/volume) was stereotaxically delivered into the ipsilateral striatum (coordinates from the Bregma: AP, 1.0 mm; ML, 2.5 mm; DV, -4.0 mm dorsoventral). The injection rate was 0.2 µL/min, and the glass pipette was left in the place for an additional 10 min before being withdrawn at a rate of 1 mm/min. The animals were sacrificed at 3 days ($n = 8$), 1 week ($n = 6$), 2 weeks ($n = 11$), and 4 weeks ($n = 7$) following a 30-min MCAO for immunostaining analysis and at 13 to 16 weeks for immunoelectron microscopy ($n = 10$) and electrophysiology recordings ($n = 7$).

Brain Section Preparation

Rats were deeply anesthetized and quickly transcardially perfused with 0.9% saline solution followed by 4% paraformaldehyde dissolved in 0.1 M phosphate-buffer (pH 7.4). The brains were removed, fixed for 6 h in 4% paraformaldehyde, and cryoprotected in buffered 30% sucrose until they sank. A freezing microtome (Jung Histocut, Model 820-II, Leica, Germany) was used to cut 30

μm thick coronal sections at levels 1.60 mm to -4.8 mm from Bregma. Sections were stored at -20°C in a cryoprotectant solution for further histological analysis.

Fluorescence Immunolabeling and Confocal Microscopy

For triple-labeling of BrdU-GFAP-*nestin/Pax6*, brain sections were obtained from rats sacrificed 3 days after MCAO. The sections were first incubated with a mouse anti-BrdU antibody (1:200, Roche, Mannheim, Germany) or rabbit polyclonal anti-BrdU antibody (1:200, Megabase, Brussels, Belgium) at 4°C overnight and then an anti-mouse/rabbit IgG-rhodamine (1:50, Santa Cruz Biotechnology, Santa Cruz, CA) secondary antibody. Then, the sections were incubated in a rabbit polyclonal anti-Pax6 (1:200, Invitrogen, Carlsbad, CA) or a mouse monoclonal anti-*nestin* (1:1,000, Sigma-Aldrich, St. Louis, MO) antibody at 4°C overnight followed by an anti-rabbit/mouse IgG-Cy5 (1:200, Abcam, Cambridge, UK) secondary antibody. Finally, the sections were incubated in a goat polyclonal anti-GFAP (1:200, Abcam, Cambridge, UK) antibody at 4°C overnight followed by an anti-goat IgG-FITC (1:500, Invitrogen, Carlsbad, CA) secondary antibody.

To trace the transdifferentiation process of GFP-expressing astrocytes, the double-labeling of GFP and stage-specific neuronal markers was performed as follows. First, brain sections at levels 1.20 mm to 0.2 mm from Bregma (based on the region of GFP expression) were incubated with a mouse monoclonal anti-GFP (1:500, Santa Cruz Biotechnology, Santa Cruz, CA) or goat polyclonal anti-GFP (1:500, Abcam, Cambridge, UK) antibody at 4°C overnight and then with anti-mouse IgG-FITC (1:50, Santa Cruz Biotechnology, Santa Cruz, CA) or anti-goat IgG-FITC secondary antibodies, respectively. The sections were then incubated in one of following primary antibodies: mouse monoclonal anti-*nestin* (1:1,000, BD Pharmingen, San Diego, CA), mouse anti- β III-tubulin (Tuj1, 1:100, Chemicon, Temecula, CA), a rabbit antibody against microtubule-associated protein 2 (MAP2) (1:200, Millipore, Billerica, MA), rabbit anti-*NeuN* (1:200, Millipore, Billerica, MA), a rabbit polyclonal antibody against glutamic acid decarboxylase (GAD67, 1:2,000, Santa Cruz Biotechnology, Santa Cruz, CA), mouse monoclonal anti-choline acetyltransferase (ChAT, 1:200, Chemicon, Temecula, CA), rabbit polyclonal anti-dopamine receptor D2-like family (D2L, 1:200, Chemicon, Temecula, CA), or rabbit polyclonal anti-N-methyl-D-aspartate receptor subunit R2 (NR2, 1:100, Chemicon, Temecula, CA) overnight at 4°C . The sections were then labeled with an anti-mouse/rabbit IgG-rhodamine secondary antibody (1:50; Santa Cruz Biotechnology, Santa Cruz, CA). After washing, the sections were mounted on glass slides and coverslipped using fluorescence mounting media. Fluorescent signals were detected using a confocal laser scanning microscope (TCS SP5, Leica, Heidelberg, Germany) at excitation and emission wavelengths of 535 and 565 nm (rhodamine), 488 and 525 nm (FITC), or 561 and 633 nm (Cy5), respectively.

Immunohistochemical Staining of GFP

To observe the morphology of GFP⁺ cells, 50 μm thick sections (the same slices were used in immunoelectron microscope experiments) were incubated with mouse monoclonal anti-GFP (1:500, Santa Cruz

Biotechnology, Santa Cruz, CA) for 48 h at 4°C followed by 4 to 6 h of blocking in 10% bovine serum. Then, the sections were incubated with biotinylated anti-mouse IgG (1:200, Vector Laboratories Inc., Burlingame, CA) at 37°C for 4 to 6 h and an avidin-biotin-peroxidase complex (1:200, Vector) at 37°C for 4 to 6 h. Immunoreactivity was visualized by 0.05% diaminobenzidine (DAB). Negative controls received identical treatment, except for the omission of primary antibodies, and showed no specific staining.

Immunoelectron Microscopy

Rats were perfused with 4% paraformaldehyde dissolved in 0.1 M phosphate-buffer (pH 7.4) containing 0.25% glutaraldehyde after 13 to 16 weeks of reperfusion after a 30-min MCAO. The pGfa2-eGFP plasmids were injected into the striatum after MCAO. Coronal sections were cut at 50- μm thickness using a vibratome and subjected to GFP immunostaining as described above. Then, GFP⁺ cells were cut under microscopic observation and embedded with Epon812 resin. The embedded samples were cut at 70-nm thickness with an ultramicrotome (LKB2088). The GFP⁺ signals on the ultrasections were visualized with lead acetate and uranyl staining, observed, and photographed with an electron microscope (JEM1200).

Electrophysiological Recording

Thirteen to 16 weeks after the surgical procedure, rats were anaesthetized with chloral hydrate (360 mg/kg, i.p.) and decapitated. The brains were quickly removed and placed in an ice-cold oxygenated slicing solution containing (in mM): 112.0 choline chloride, 2.5 KCl, 1.3 NaH_2PO_4 , 26.0 NaHCO_3 , 0.5 CaCl_2 , 7.0 MgCl_2 , 25.0 dextrose, and 1.5 sodium ascorbate. Vibratome-cut slices (200–250 μm thick) were transferred into a slice storage chamber filled with artificial cerebrospinal fluid (ACSF) composed of the following (in mM): 124.0 NaCl, 2.5 KCl, 1.2 NaH_2PO_4 , 26.0 NaHCO_3 , 2 CaCl_2 , 1.3 MgCl_2 , and 10 glucose. The slices were continuously oxygenated with 95% O_2 –5% CO_2 (pH 7.4) and maintained at 22 to 24°C for 1 h. Microelectrodes (3–4 M Ω) were filled with intracellular solution containing (in mM, pH7.25): 135 KCl, 2 $\text{MgSO}_4\cdot 7\text{H}_2\text{O}$, 0.1 CaCl_2 , 1.1 EGTA, 2 K_2ATP , 0.1 Na_3GTP , and 10 HEPES. Lucifer yellow (1 mM) was included in the intracellular solution for visual identification of the recorded cells.

Cells showing neuronal morphology in the striatal slices were selected for electrophysiological recordings. Whole-cell recordings were performed at room temperature with an Axopatch 700B amplifier, digitized with a Digidata 1322A (Molecular Devices) and acquired onto a PC using Clampex 9.0 software (Axon Instruments). In all recordings, the series resistance (typically 15–30 M Ω) and membrane capacitance were observed but not compensated. After the formation of a gigaseal, the whole-cell mode was established with gentle negative suction. The resting membrane potential and membrane capacitance were measured immediately after rupture of the patch membrane. The input resistance was calculated from the steady-state voltage response evoked by a small hyperpolarizing DC current pulse (-2 mV, 50 ms) from a holding potential of -70 mV. The inverse of the inter-spike interval between the first two spikes of the train was calculated as the firing rate. Action potentials were recorded in the current clamp configuration from -400 to

+150 pA with 50 pA steps and a 2 s duration per pulse. Spontaneous postsynaptic currents were recorded at a holding potential of -70 mV. Inward and outward currents were elicited in the voltage clamp configuration from -70 mV to $+50$ mV at 20 mV steps with a duration of 300 ms per pulse.

After recording, slices were fixed in 4% paraformaldehyde at 4°C overnight, followed by incubation with a mouse monoclonal anti-GFP (1:500, Santa Cruz Biotechnology, Santa Cruz, CA) primary antibody and then an anti-mouse IgG-rhodamine (1:50, Santa Cruz Biotechnology, Santa Cruz, CA) secondary antibody. GFP-negative neurons were recorded as controls. Fluorescent signals were detected by confocal laser scanning microscopy at excitation and emission wavelengths of 535 and 565 nm (rhodamine) and 488 and 525 nm (Lucifer yellow), respectively.

Data Analysis

All data are expressed as the means \pm SEM and were analyzed using unpaired Student *t*-tests for two-group comparisons and one-way analysis of variance with a *post hoc* least significant difference and Tukey's test for multiple comparisons. A value of $P < 0.05$ was considered statistically significant.

Results

Cerebral Ischemia Induces Pax6 Expression in Reactive Astrocytes After MCAO

As expected, cerebral ischemic injury could cause activation of astrocytes in injured brain regions. We observed that reactive astrocytes in the ischemic penumbra of the ipsilateral striatum showed hypertrophic cell somata and processes along with high levels of GFAP (GFAP⁺) expression 3 days after MCAO. Reactive astrocytes also proliferated following injury as demonstrated by double-staining of GFAP and BrdU (GFAP⁺-BrdU⁺). We found that these proliferating astrocytes also expressed nestin (GFAP⁺-BrdU⁺-Nestin⁺) or Pax6 (GFAP⁺-BrdU⁺-Pax6⁺), a marker of neural stem/progenitor cells and a transcription factor of neuronal fate determinant, respectively (Fig. 1A–D). To determine the number of astrocytes that expressed Pax6, we used immunohistochemical methods to double-stain GFAP and Pax6 (GFAP⁺-Pax6⁺) as shown in Fig. 1E. We found that ischemic injury significantly increased the number of GFAP⁺-Pax6⁺ cells (Fig. 1F). These results provide additional support for the idea that striatal reactive astrocytes possess the potential to re-enter the cell division cycle and transdifferentiate into neural stem/progenitor cells following ischemic injury. We next asked whether these resident astrocytes could be transdifferentiated *in vivo* into mature and functional neurons in the ischemically injured striatum.

pGfa2-eGFP Injection Traces Transdifferentiation of Resident Reactive Astrocytes into Neural Stem/Progenitor Cells

We injected pGfa2-eGFP plasmids that express eGFP (GFP) driven by the human GFAP promoter into the striatum

ipsilateral to a MCAO to label resident reactive astrocytes based on the protocols (Fig. 2A,B). We also performed single immunostaining of rat brain sections from different time points after MCAO to further enhance the GFP signals and scanned the fluorescent signals under a confocal laser microscope. As shown in Fig. 2C, 3 days after plasmid injection, GFP positive (GFP⁺) signals were detected in the ipsilateral striatum along the needle tract. We also observed that the GFP⁺ signals spread 640.14 ± 96 μm away from the injection site in brain sections at levels 1.20 mm to 0.2 mm from Bregma. The GFP⁺ cells showed mostly glial-like cell morphology 3 days after the injection. More interestingly, some GFP⁺ cells gradually showed neuron-like morphology in the ischemically injured brain from 7 days after MCAO. The GFP⁺ signals could still be detected even at 13 weeks, although the density of the signals was reduced (Fig. 2C). Double immunostaining showed that 86% of the GFP⁺ cells (509 GFP⁺ cells) that bordered the ischemic core were co-stained with a GFAP (GFP⁺-GFAP⁺), and 47% were co-stained with nestin (GFP⁺-Nestin⁺) at 3 days postinjection (Figs. 2D,E and 3A–b,I). We also found that some of the GFP⁺ cells were co-stained with the stem cell markers Sox2 (GFP⁺-Sox2⁺) and Pax6 (GFP⁺-Pax6⁺), as shown in Fig. 2F,G. These results suggest that striatal injection of pGfa2-eGFP can be used to trace the transdifferentiation of resident reactive astrocytes into neural stem/progenitor cells.

Striatal Resident GFP⁺ Astrocytes Express Neural Lineage Markers After MCAO

To determine whether striatal GFP⁺ astrocytes could become new neurons, we performed triple staining of GFAP, NeuN and GFP in brain sections at 3 days and 2 weeks after MCAO. We found that, at 3 days, GFP was mostly expressed in the astrocytes because GFP⁺ signals were only observed in GFAP⁺ cells and not in NeuN⁺ cells (Fig. 2H–J). At 2 weeks after MCAO, some of GFP⁺ signals could still be detected in the GFAP⁺ astrocytes. However, other signals were detected in the NeuN⁺ neurons (Fig. 2K–M). Meanwhile, we observed that no cell showed triple staining of GFAP, NeuN and GFP as shown in Fig. 2H–M. Therefore, in the following study, we performed double-staining for GFP and either nestin, Tuj1, MAP-2, or NeuN to trace the neural fate of reactive astrocytes. Taking into account the pGfa2-eGFP plasmids expression time and the timing of astrogliosis and neurogenesis after brain injury (Jin et al., 2001; Robel et al., 2011; Wang et al., 2007), we collected brains sections at 3, 7, 14, and 28 days after MCAO as indicated in the experimental protocols (Fig. 2A). We found that resident GFP⁺ cells in the ischemically injured striatum showed time-dependent morphological changes along with expression of proteins specific for neuronal lineage. At 3 days

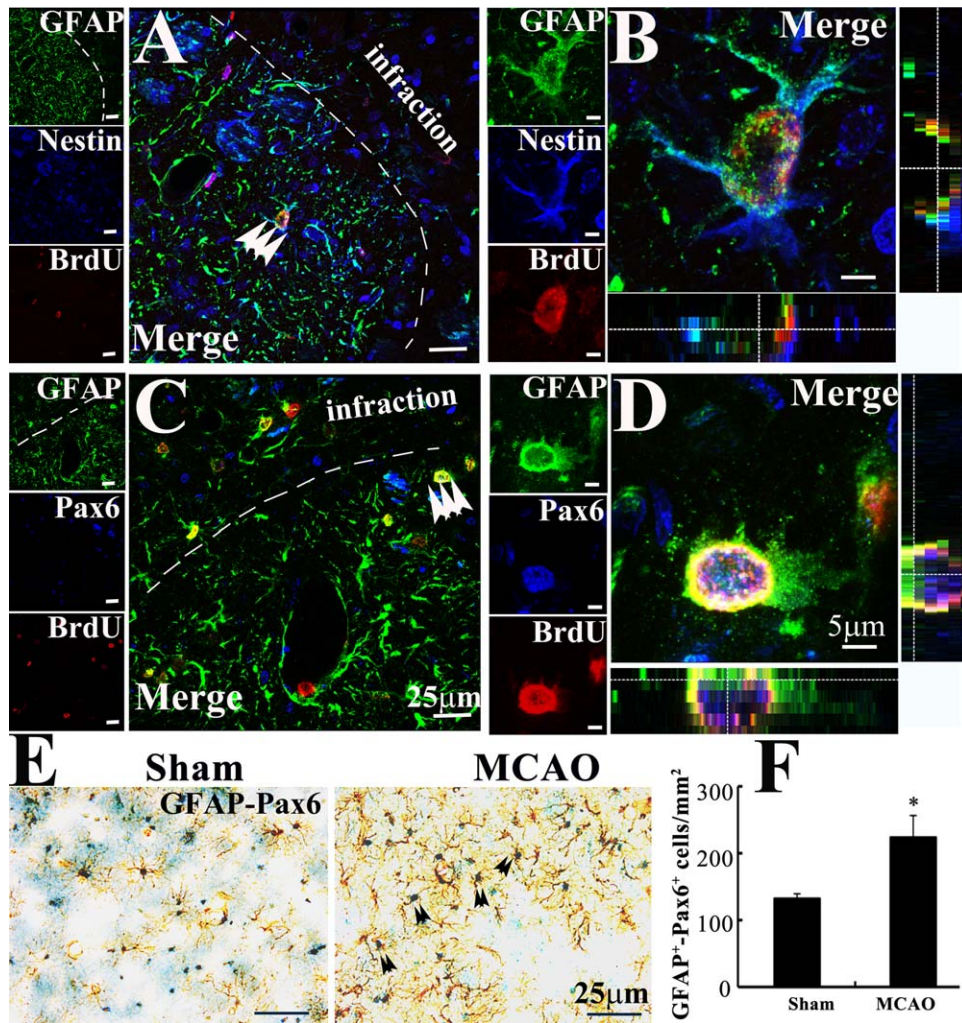


FIGURE 1: Co-expression of GFAP with the neural stem/progenitor cell markers nestin or Pax6 in the ischemic striatum. (A, C) Immunofluorescence images show GFAP⁺-Nestin⁺ (A) and GFAP⁺-Pax6⁺ (C) reactive astrocytes in peri-infarctions of the ipsilateral striatum at 3 days after MCAO. A subpopulation of GFAP⁺-Nestin⁺ or GFAP⁺-Pax6⁺ cells were labeled by BrdU (a marker of proliferative cells) as shown by the white triple arrowheads. (B, D) Higher power fields with an orthogonal view of a confocal z-stack illustrate the triple-labeling of GFAP⁺-Nestin⁺-BrdU⁺ (B) or GFAP⁺-Pax6⁺-BrdU⁺ (D) from A and C, respectively. (E, F) The change in the number of GFAP⁺-Pax6⁺ cells in response to ischemic injury is shown; GFAP⁺-Pax6⁺ cells are indicated by double arrowheads (E). Scale bars = 25 μm (A, C, E); Scale bars = 5 μm (B, D). (n = 5, *P < 0.05; Fig. 1F).

after MCAO, we detected that 47% of GFP⁺ cells were co-stained with nestin, as mentioned above. Interestingly, starting from 7 days after stroke, we found that some GFP⁺ cells showed neuron-like morphology. Multiple immunostaining results showed that 6-8.5% of GFP⁺ cells co-stained with Tuj1 (GFP⁺-Tuj-1⁺), an immature neuronal marker (Fig. 3C,D). Four weeks (28 days) after MCAO, GFP⁺-Tuj-1⁺ cells could still be detected, but the number of these cells was reduced (Fig. 3I). Meanwhile, we found that some GFP⁺ cells showed double-staining with NeuN (GFP⁺-NeuN⁺) or MAP-2 (GFP⁺-MAP-2⁺), markers of mature neurons, at 2 and 4 weeks after MCAO (Fig. 3E-H). Statistical analysis indicated that 12 to 14% of GFP⁺ cells showed MAP-2⁺. These results indicated that striatal resident reactive astrocytes

could transdifferentiate into mature neurons *in vivo* in response to cerebral ischemic injury.

Astrocyte-Derived Neurons Morphologically Integrate with Other Neurons

The next question we sought to answer was whether resident astrocyte-derived neurons could differentiate into morphologically mature and functional neurons. Therefore, we collected brain sections for detection of neurotransmitter synthetic enzymes and receptors. At this time point, we found expression of the ChAT, GAD67, D2L, and NR2 proteins in the GFP⁺ cells (Fig. 4A-D). These results suggest that GFP⁺ neurons can develop into either cholinergic or GABAergic neurons, and their membranes can express dopamine and glutamate receptors.

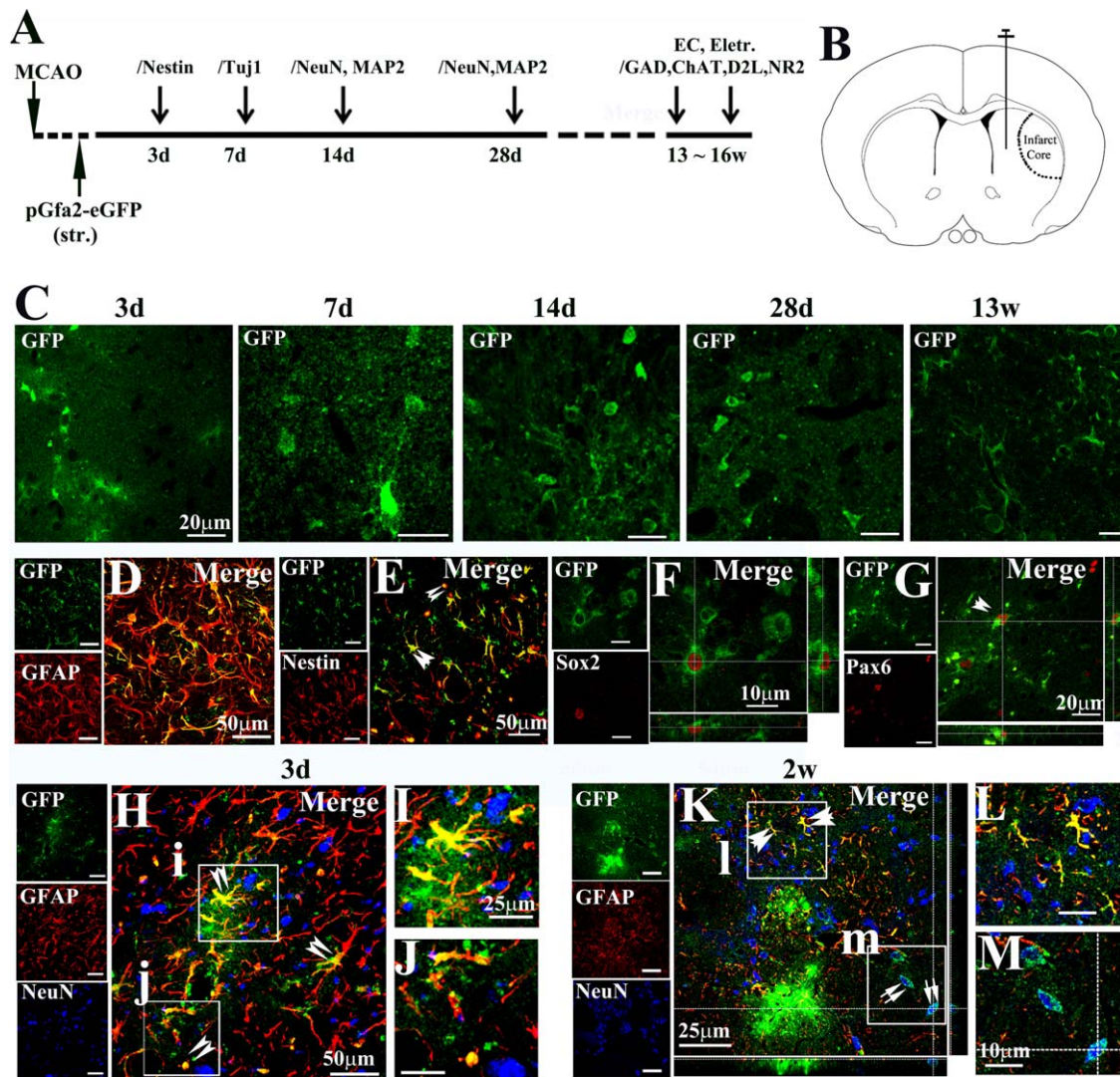


FIGURE 2: Identification of GFP signals after pGfa2-eGFP plasmid microinjection following transient MCAO. (A, B) Illustration of experimental protocol. Animals were sacrificed at 3, 7, 14, and 28 days (d) or 13 to 16 weeks (w) ($n \geq 6$ per time) after MCAO. The pGfa2-eGFP plasmids were stereotaxically injected into the ipsilateral striatum following a 30-min MCAO (B). (C) Image of GFP-positive cells close to the injection site at different times after MCAO. (D) Most of the GFP⁺ cells co-localize with GFAP at 3 days after MCAO. (E–G) Neural stem/progenitor cell markers (nestin (E), Sox2 (F), Pax6 (G)) co-expressed in GFP⁺ cells; (H) most of GFP⁺ cells co-expressed GFAP but not NeuN at 3 days after MCAO (indicated by double arrowheads). I and J are magnified views of H-i and H-j. (K–M) At 2 weeks after stroke, some of GFP⁺ cells coexpressed NeuN (indicated by double arrows in K-m, M), and others still co-localized with GFAP (indicated by double arrowheads in K-l, L). L and M are magnified views of K-l and K-m. Scale bars = 20 μm (C, G); Scale bars = 50 μm (D, E, H); Scale bars = 10 μm (F, L, M); Scale bars = 25 μm (I, J, K).

Then, we performed immunohistochemical staining with sections from rats at 13 weeks after MCAO to reveal the dendritic process of GFP⁺ cells (Fig. 4E–H). We observed different GFP⁺ cell morphologies under microscopic observation (Fig. 4E). Some GFP⁺ cells retained an astroglial-like morphology (Fig. 4F), but others showed very typical neuron-like morphology with neural polarity, indicated by a rounded large cell body with neurites and dendritic branches (Fig. 4G,H). We also noticed that a few GFP⁺ cells had small cell bodies without processes and did not look like astroglial cells or neurons (Fig. 4E–G).

We next used electron microscopy to analyze the ultrastructure of the transdifferentiated GFP⁺ cells. The ultrastructural images showed GFP⁺ neuronal cell bodies (Fig. 5D), GFP⁺ neural dendrites (Fig. 5A,B), and typical synaptic structures (Fig. 5C,E). We also noticed both symmetric and asymmetric GFP⁺ synapses, which connected with pre-existing (Fig. 5E) and newly formed neurons (Fig. 5C). These results indicated that newly generated neurons derived from reactive astrocytes following ischemic injury could form new synapses. The present results provided a morphological basis for the re-establishment of neural networks. Thus we next

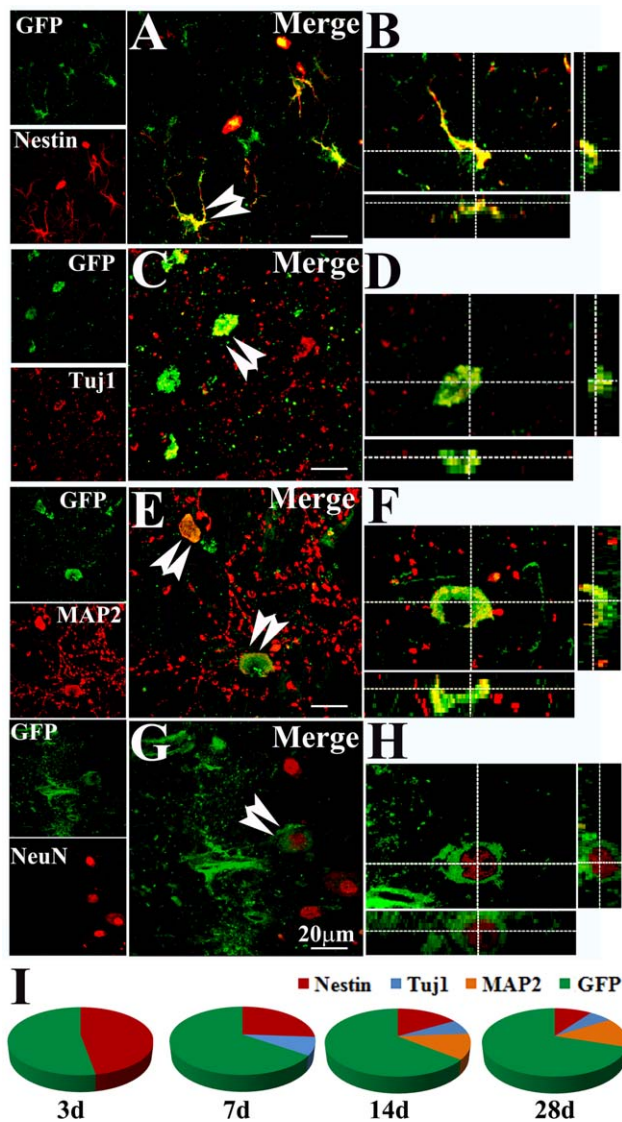


FIGURE 3: A subpopulation of GFP-traced astrocytes gradually transformed into neurons during reperfusion after MCAO. (A–H) Immunofluorescence images showed co-expression of GFP with the stage-specific neuronal markers nestin (A), Tuj1 (C), MAP2 (E) and NeuN (G). Double-labeling is indicated with white double-arrowheads and was confirmed by confocal images of a z-stack (B, D, F and H, respectively). (I) The percentage of GFP⁺ cells that were co-labeled with a neuronal marker (nestin, Tuj1, MAP2) at different days (d) after MCAO is shown. Scale bars = 20 μ m (A–L).

asked whether these GFP⁺ neurons were electrophysiologically functional.

Striatal Astrocyte-Derived New Neurons Functionally Integrate into Local Neural Networks

We next assessed whether these newly generated neurons could become functionally integrated into neural networks. To test this, we performed whole-cell patch-clamp recordings from GFP^{+/−} neuron-like cells in freshly prepared striatal slices from rat brains between 13 and 16 weeks after MCAO.

To confirm that the recorded neurons were newly generated, we filled them with Lucifer yellow dye while recording and performed immunostaining after recording to distinguish GFP fluorescence from the Lucifer yellow dye. One hundred and one cells were patched for electrophysiological recordings in acute striatal slices. We classified the recorded cells as GFP⁺ ($n = 27$) and GFP[−] neurons ($n = 74$) based on GFP immunostaining. During the recording, we also found that depolarizing current pulses could not elicit action potentials (AP) in nine of the recorded GFP⁺ cells. Therefore, we further classified the GFP⁺ cells as AP⁺-GFP⁺ ($n = 18$) and AP[−]-GFP⁺ ($n = 9$) cells.

In the example shown in Fig. 6, cell-a (AP⁺-GFP⁺) and cell-b (AP[−]-GFP⁺) were newly generated cells as indicated by double-labeling with Lucifer yellow and GFP (Fig. 6A,B), whereas cell-c (GFP[−]) was a pre-existing neuron as it was only labeled with Lucifer yellow (Fig. 6A). Figures 6C–E and 6F–H show representative electrophysiological activities corresponding to cell-a and cell-b in Fig. 6A,B, respectively. Under voltage clamp at a holding potential of -70 mV, both cell-a and cell-c exhibited active and sharp spontaneous postsynaptic currents (sPSCs) with rapid onsets (less than 1 ms) and slow exponential decays, indicating typical fast postsynaptic responses to fast neurotransmitters (Fig. 6C). However, cell-b showed constant spontaneous currents, and the amplitude of the currents did not change significantly during the recording (Fig. 6F). In the current clamp configuration, while stepping from -400 pA to 150 pA with 50 pA steps, we found that suprathreshold depolarizing current pulses elicited repetitive action potentials, whereas negative current pulses produced hyperpolarized membrane potentials in both cell-a (Fig. 6D) and cell-c (pre-existing neuron, data not shown). However, neither the same current stimulation nor even higher depolarizing currents could induce action potentials in cell-b, which only showed a steady linear current–voltage relationship (Fig. 6G). Membrane currents were recorded in the voltage clamp configuration in 20 mV steps from -70 mV to 50 mV. We recorded fast and large inward (-4.213 nA) and outward currents in cell-a (Fig. 6E). However, we could only record very small and slow inward and outward currents in cell-b (Fig. 6H). The electrophysiological parameters of the recorded cells for the three cell groups showed lower input resistances and higher membrane potentials for the cell-b type neurons than for the cell-a and cell-c type neurons (summarized in Table 1).

After recording, we immunostained neurons with a secondary antibody conjugated with rhodamine to distinguish GFP signals from the Lucifer yellow dye and observed the fluorescent signals of GFP (Rhodamine, red color) and Lucifer yellow (green color) using a confocal microscope. We observed that the cell-b type cells mostly showed many highly

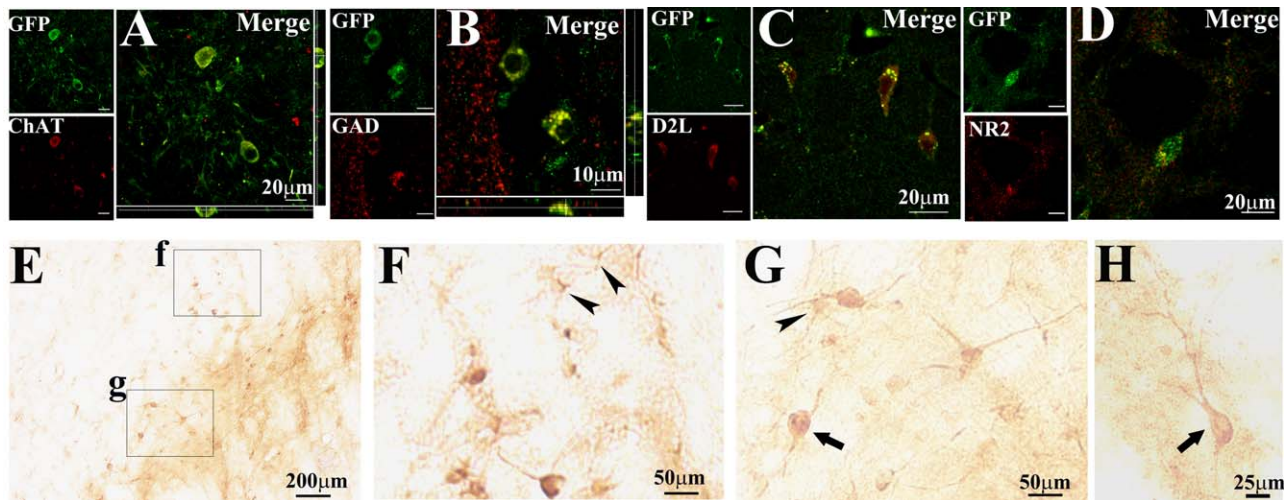


FIGURE 4: GFP-positive cells displayed mature neuronal features at 13 weeks after MCAO. (A–D) Immunofluorescence double-staining photos showed co-localization of GFP with the mature neuronal markers ChAT (A) and GAD (B), as well as the receptors D2L (C) and NR2 (D). (E) A low power photograph (light microscopy with a 10× objective) revealed GFP signals in the boundary of the infarct. Both astrocytic (indicated by arrowheads in F and G) and neuronal GFP⁺ cells (indicated by arrows in G) could be detected around injection sites within the ischemic striatum. Photos F and G are magnified views of E-f and E-g. (H) Immunohistochemical single-labeling of GFP showed neuronal specific neurite structures. Scale bars = 20 μm (A, C, D); scale bar = 10 μm (B); scale bar = 200 μm (E); scale bars = 50 μm (F–G); scale bar = 25 μm (H).

branched processes (similar to protoplasmic astrocytes), whereas the cell-a type cells usually showed two or three branches (similar to neurons). Combining the electrophysiological recordings with the morphological data, we found that the cell-a and cell-c (pre-existing neurons) type cells possessed typical neuronal morphology and electrophysiological activity, whereas the cell-b type cells showed astrocytic properties.

Discussion

This study provides the first evidence that striatal resident reactive astrocytes can transdifferentiate into functional mature neurons in adult mammalian brains *in vivo* in response to ischemic injury. These astrocyte-derived new neurons form GABAergic and cholinergic neurons, express glutamate and dopamine receptors, form neural polarity, and make synapses—the morphological basis for receiving synaptic inputs from surrounding neurons. Electrophysiological recordings combined with histological confirmation in acute brain slices indicate that these striatal resident astrocyte-derived neurons can also fire action potentials and display spontaneous postsynaptic currents. Thus, these new neurons can form synapses with pre-existing neurons and functionally integrate into local neural networks. The results of this study expand our knowledge of how reactive astrocytes play important roles in brain repair in the adult mammalian brain in response to ischemic injury. They also help us to understand the cellular mechanisms of adult neurogenesis.

Consistent with previous results (Liu et al., 2002; Pekny and Nilsson, 2005), the present study indicates that astrocytes

can be activated after ischemic injury in the adult brain. Additionally, our evidence further suggests that a portion of these reactive astrocytes transform into neural stem-like cells with multipotent and proliferative characteristics because

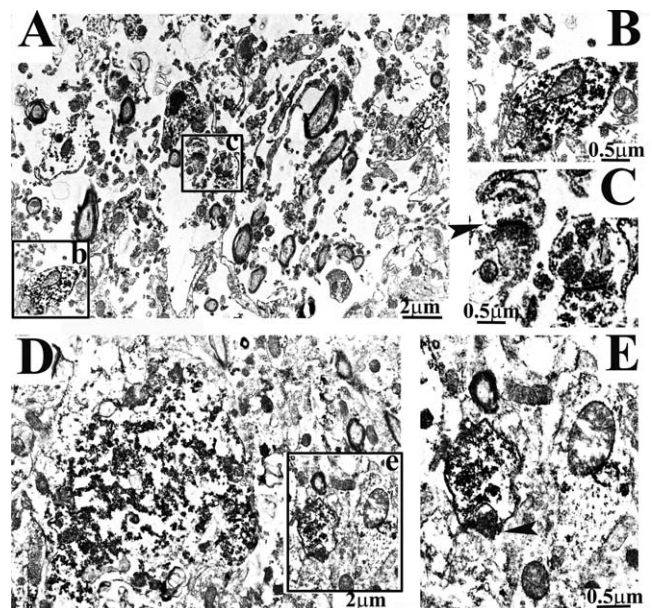


FIGURE 5: Immunoelectron microscopy revealed GFP-expressing dendrites and synapse ultrastructures in the ipsilateral striatum at 13 to 16 weeks after MCAO. Electron microscopy photographs showed fields with GFP signals (A), GFP-positive dendrites (B), synapses (C, E) (illustrated by an arrowhead), a GFP-positive cell body and the surrounding presynaptic synapse (D). B, C, and E are magnified views of A-b, A-c, and D-e, respectively. Scale bars = 2 μm (A, D) and 0.5 μm (B, C, and E).

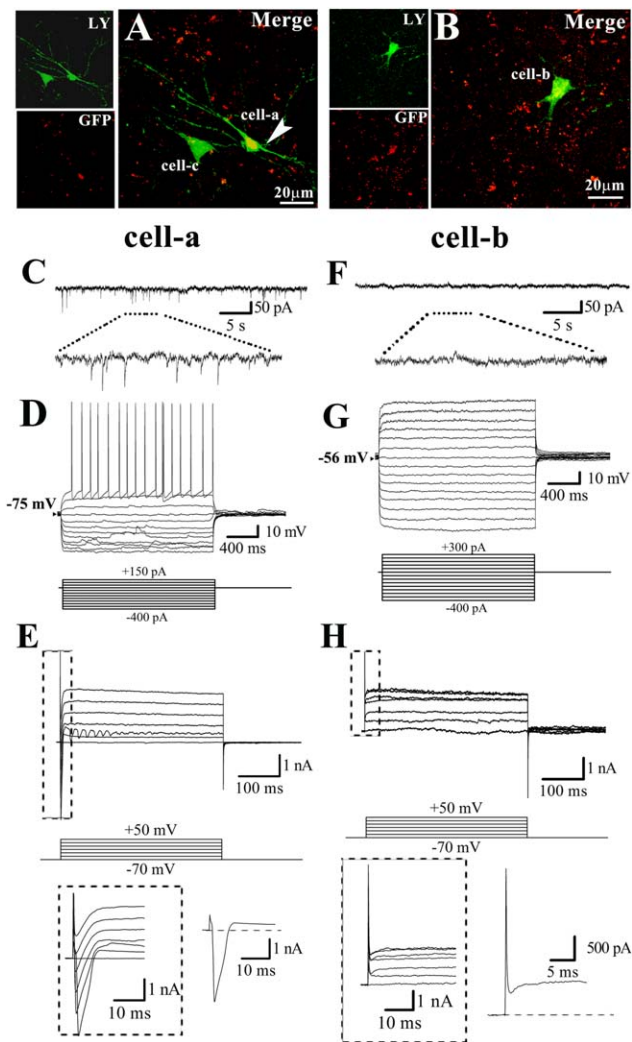


FIGURE 6: GFP⁺ cells display electrophysiological properties 13 to 16 weeks after MCAO. (A, B) Confocal microscope images of brain slices with GFP antibody enhancement following electrophysiological recordings. A pre-existing cell was GFP negative and filled with Lucifer yellow dye during recording (cell-c, A), while newly generated cells were double-labeled with GFP and Lucifer yellow (cell-a, A and cell-b, B). (C, F) Representative traces of postsynaptic currents recorded in GFP⁺ cell-a and cell-b. (D, G) A train of action potentials was elicited by depolarizing currents in cell-a in the current-clamp mode (−400 to +150 pA, step 50 pA, 2 s), but not in cell-b with even higher depolarizing currents (−400 to +300 pA, step 50 pA, 2 s). (E, H) Analysis of voltage gated currents in GFP⁺ cells recorded in voltage-clamp mode (from −70 mV to +50 mV, step 20 mV). The representative single trace was elicited at a voltage of −30 mV. The recording data show a larger inward current in cell-a (E) and a smaller inward current in cell-b (H). Scale bars = 20 μm (A, B).

some GFAP⁺-BrdU[±] cells were co-labeled for nestin, a marker of neural stem/progenitor cells (Fig. 1A,B). Pax6, a transcription factor of neuronal fate determinant (Hack et al., 2005; Heins et al., 2002; Jang and Goldman, 2011; Kronenberg et al., 2010), is expressed in radial glia on the ventricular surface (Englund et al., 2005) and astroglial cells in the adult

SVZ, which is a neurogenic region (Jang and Goldman, 2011), as well as in immature or mature astrocytes (Sakurai and Osumi, 2008). Exogenous overexpression of Pax6 in the glial cells evokes transdifferentiation of astrocytes into neuroblasts (Kronenberg et al., 2010). We found that endogenous Pax6, which is highly expressed in striatal reactive astrocytes, could be significantly enhanced by ischemic injury (Fig. 1E,F). Taken together, our data further suggest that these endogenous reactive astrocytes possess the potential to transdifferentiate into neuroprogenitors. When we microinjected GFAP promoter-controlled eGFP (pGfa2-eGFP plasmids) into the striatum ipsilateral to a MCAO and traced the neural fate of reactive astrocytes in response to ischemic stroke, we found that the GFP⁺ astrocytes could further transdifferentiate into neurons after stroke as indicated by double GFP⁺-Tuj-1⁺, GFP⁺-NeuN⁺, and GFP⁺-MAP-2⁺ stained cells (Fig. 3C–H). The present results clearly demonstrate that striatal endogenous reactive astrocytes can transdifferentiate into new neurons in response to ischemic injury, which is consistent with recent findings (Magnusson et al., 2014).

For these newly generated neurons to participate in brain repair after injury, they have to be functional. In the present study, we found several pieces of evidence supporting the idea that astrocyte-derived neurons could also become functional neurons. First, astrocyte-derived neurons expressed neurotransmitter-synthesizing enzymes, such as choline acetyltransferase and glutamic acid decarboxylase, as indicated by the GFP⁺-GAD67⁺ and GFP⁺-ChAT⁺ cells in Fig. 4A,B. This result suggested that these astrocyte-derived neurons could become regionally appropriate GABAergic and cholinergic neurons. Second, astrocyte-derived neurons expressed the D2L dopamine receptor and the NR2 glutamate receptor on their membranes (Fig. 4C,D), which provides the ability to receive presynaptic inputs. Third, single immunostaining and electron microscopy analysis indicated that GFP⁺ neurons developed neurites with several branches (Fig. 4E–H) and formed dendrites and synapses (Fig. 5). Fourth, astrocyte-derived neurons showed electrophysiological characteristics of mature neurons as indicated in Table 1 and Fig. 6, cell-a. For example, GFP⁺ neuron-like cells (cell-a in Fig. 6A,C–E) could fire action potentials under current clamp conditions and had active spontaneous postsynaptic currents at a holding potential of −70 mV, indicating that cell-a type cells are functional neurons that possess the ability to fire action potentials and response to synaptic inputs. However, GFP⁺ astrocyte-like cells (cell-b in Fig. 6B,F–H) showed relatively passive spontaneous postsynaptic currents and could not be elicited to fire action potentials; these properties are similar to the typical electrophysiological activity detected in cultured mature astrocytes, as previously reported (Berninger et al., 2007). Collectively, the findings of the present study

TABLE 1: Comparison of Electrophysiological Parameters of GFP⁺ and GFP⁻ Neurons in Striatal Adult Rat Brain Slices 13 to 16 Weeks After MCAO

Groups	GFP ⁻ cells	GFP ⁺ cells	
		AP ⁺ /GFP ⁺ cells	AP ⁻ /GFP ⁺ cells
Cell number	74	18	9
Membrane capacitance (pF)	63.83 ± 3.42	52.86 ± 6.39	29.21 ± 3.87†
Input resistance (MΩ)	143.21 ± 20.35	122.60 ± 12.38*	24.67 ± 8.32†
Resting potential (mV)	-70.67 ± 2.35	-68.85 ± 2.98	-42.35 ± 6.56†
Spiking threshold (mV)	-42.59 ± 1.71	-43.89 ± 1.37	NO
Firing frequency (Hz)	14.06 ± 1.56	12.45 ± 2.04	NO
Spontaneous activity (Hz)	1.73 ± 0.82	0.93 ± 0.73	NO

Experiments on GFP⁺ cells ($n = 27$) were conducted 13 weeks after MCAO. The pre-existing cells (GFP⁻, $n = 74$) were analyzed as a control group. Input resistance was calculated by measuring the steady-state passive current evoked with a hyperpolarizing pulse with an amplitude of 2 mV and a duration of 5 ms from a holding potential of -70 mV in the voltage clamp mode. The spike threshold was measured as the voltage difference between the resting membrane potential and spike onset. The spike frequency was calculated as the inverse of the inter-spike interval between the first two spikes of the train in response to a 150 pA depolarizing current step during recording. The data are reported as the means ± SEM.

* $P < 0.05$ versus the GFP⁻ group.

† $P < 0.05$ versus the AP⁺-GFP⁺ group.

reveal that resident astrocyte-derived neurons in the ischemically injured striatum can develop into morphological and functional mature neurons and further participate in the reconstruction of regional neural networks.

We noted several contradictory results, including that endogenous astrocytes themselves have no capability to differentiate into neurons in the non-neurogenic regions of adult brains, even in cells have become neuroblasts (Buffo et al., 2008; Niu et al., 2013). This contrasting phenomenon might be caused by several factors. (1). Different experimental models or brain regions might have specific intrinsic mechanisms that control the transdifferentiation of astrocytes. We used the same cerebral ischemic injury model and examined identical brain regions to those reported by Magnusson et al. (2014), which were different from the experimental protocols reported by Buffo, who traced fate mapping of astrocytes using viral injection of glutamate aspartate transporter (GLAST) promoter-targeted β -galactosidase (β -gal) into cortical regions in a stab wound model (Buffo et al., 2008). (2). Cerebral injury could stimulate the activation of endogenous neurogenic transcription factors in the brain to direct reactive astrocytes to transdifferentiate into neurons, which does not occur in intact adult brains. For example, we found that ischemic injury could induce astrocytes to increase expression of Pax6, a neural transcription factor (Fig. 1). Moreover, inhibition of notch-1 signaling could further increase the capability of neural transdifferentiation of astrocytes in ischemically injured brains (Magnusson et al., 2014). In contrast, striatal

astrocytes in intact adult brains normally do not undergo neural transdifferentiation. However, neural transdifferentiation from astrocytes could be observed in brains after exogenous overexpression of neural transcription factors (Kronenberg et al., 2010; Niu et al., 2013). The results suggest that ischemically injured, but not intact, brains can activate endogenous mechanisms to redirect astrocyte transdifferentiation into neurons.

Nevertheless, we also noticed that only approximately 12 to 14% of reactive astrocytes could become new mature neurons (Fig. 3), which was constant with the previous reports (Kronenberg et al., 2010; Magnusson et al., 2014; Niu et al., 2013). Most cells underwent astrogliosis. Based on present knowledge, the function of astroglial cells in the damaged brain is very complex and includes beneficial and detrimental effects on brain repair (Buffo et al., 2010). Astrocytes synthesize and release several growth factors to enhance neurogenesis (Bath et al., 2012; Matsuoka et al., 2003; Wang et al., 2007, 2009). However, they also express several inhibitory factors that block or reduce adult neurogenesis and accelerate the formation of glial scars in the injured brain (Boda and Buffo, 2010). Therefore, it is a reasonable goal to determine a method to enhance brain repair by increasing the capacity of astrocytes to be transdifferentiated into new neurons. In the future, exogenous protein manipulation could improve the neurogenesis capacity of reactive astrocytes, which could in turn greatly benefit brain repair after stroke.

Acknowledgment

Grant sponsor: National Nature Science Foundation of China; Grant numbers: 81030020 and 30770660; Grant sponsor: National Basic Research Program of China; Grant number: 2006 CB943702; Grant sponsor: National Education Program of China; Grant number: J0730860

The authors sincerely thank Ya-Lin Huang for her excellent technical assistance.

References

- Alvarez-Buylla A, Herrera DG, Wichterle H. 2000. The subventricular zone: Source of neuronal precursors for brain repair. *Prog Brain Res* 127: 1–11.
- Arvidsson A, Collin T, Kirik D, Kokaia Z, Lindvall O. 2002. Neuronal replacement from endogenous precursors in the adult brain after stroke. *Nat Med* 8: 963–970.
- Bath KG, Akins MR, Lee FS. 2012. BDNF control of adult SVZ neurogenesis. *Dev Psychobiol* 54:578–589.
- Berninger B, Costa MR, Koch U, Schroeder T, Sutor B, Grothe B, Gotz M. 2007. Functional properties of neurons derived from in vitro reprogrammed postnatal astroglia. *J Neurosci* 27:8654–8664.
- Boda E, Buffo A. 2010. Glial cells in non-germinal territories: Insights into their stem/progenitor properties in the intact and injured nervous tissue. *Arch Ital Biol* 148:119–136.
- Buffo A, Rite I, Tripathi P, Lepier A, Colak D, Horn AP, Mori T, Gotz M. 2008. Origin and progeny of reactive gliosis: A source of multipotent cells in the injured brain. *Proc Natl Acad Sci USA* 105:3581–3586.
- Buffo A, Rolando C, Ceruti S. 2010. Astrocytes in the damaged brain: Molecular and cellular insights into their reactive response and healing potential. *Biochem Pharmacol* 79:77–89.
- Dirnagl U, Simon RP, Hallenbeck JM. 2003. Ischemic tolerance and endogenous neuroprotection. *Trends Neurosci* 26:248–254.
- Englund C, Fink A, Lau C, Pham D, Daza RA, Bulfone A, Kowalczyk T, Hevner RF. 2005. Pax6, tbr2, and tbr1 are expressed sequentially by radial glia, intermediate progenitor cells, and postmitotic neurons in developing neocortex. *J Neurosci* 25:247–251.
- Graham SH, Chen J. 2001. Programmed cell death in cerebral ischemia. *J Cereb Blood Flow Metab* 21:99–109.
- Guo JJ, Liu F, Sun X, Huang JJ, Xu M, Sun FY. 2012. Bcl-2 enhances the formation of newborn striatal long-projection neurons in adult rat brain after a transient ischemic stroke. *Neurosci Bull* 28:669–679.
- Hack MA, Saghatelian A, de Chevigny A, Pfeifer A, Ashery-Padan R, Lledo PM, Gotz M. 2005. Neuronal fate determinants of adult olfactory bulb neurogenesis. *Nat Neurosci* 8:865–872.
- Heins N, Malatesta P, Cecconi F, Nakafuku M, Tucker KL, Hack MA, Chapouton P, Barde YA, Gotz M. 2002. Glial cells generate neurons: The role of the transcription factor pax6. *Nat Neurosci* 5:308–315.
- Hou SW, Wang YQ, Xu M, Shen DH, Wang JJ, Huang F, Yu Z, Sun FY. 2008. Functional integration of newly generated neurons into striatum after cerebral ischemia in the adult rat brain. *Stroke* 39:2837–2844.
- Jang ES, Goldman JE. 2011. Pax6 expression is sufficient to induce a neurogenic fate in glial progenitors of the neonatal subventricular zone. *PLoS One* 6:e20894.
- Jin K, Minami M, Lan JQ, Mao XO, Bateur S, Simon RP, Greenberg DA. 2001. Neurogenesis in dentate subgranular zone and rostral subventricular zone after focal cerebral ischemia in the rat. *Proc Natl Acad Sci USA* 98: 4710–4715.
- Kronenberg G, Gertz K, Cheung G, Buffo A, Kettenmann H, Gotz M, Endres M. 2010. Modulation of fate determinants olig2 and pax6 in resident glia evokes spiking neuroblasts in a model of mild brain ischemia. *Stroke* 41: 2944–2949.
- Li L, Harms KM, Ventura PB, Lagace DC, Eisch AJ, Cunningham LA. 2010. Focal cerebral ischemia induces a multilineage cytogenic response from adult subventricular zone that is predominantly gliogenic. *Glia* 58:1610–1619.
- Lipton P. 1999. Ischemic cell death in brain neurons. *Physiol Rev* 79:1431–1568.
- Liu PC, Lu SD, Huang YL, Sun FY. 2002. [The expression of nestin in ischemia-injured brain of adult rat]. *Sheng Li Xue Bao* 54:294–399.
- Liu PC, Yang ZJ, Qiu MH, Zhang LM, Sun FY. 2003. Induction of CRMP-4 in striatum of adult rat after transient brain ischemia. *Acta Pharmacol Sin* 24: 1205–1211.
- Longa EZ, Weinstein PR, Carlson S, Cummins R. 1989. Reversible middle cerebral artery occlusion without craniectomy in rats. *Stroke* 20:84–91.
- Magnusson JP, Göritz C, Tatarishvili J, Dias DO, Smith EMK, Lindvall O, Kokaia Z, Frisén J. 2014. A latent neurogenic program in astrocytes regulated by notch signaling in the mouse. *Science* 346:237–241.
- Matsuoka N, Nozaki K, Takagi Y, Nishimura M, Hayashi J, Miyatake S, Hashimoto N. 2003. Adenovirus-mediated gene transfer of fibroblast growth factor-2 increases BrdU-positive cells after forebrain ischemia in gerbils. *Stroke* 34:1519–1525.
- Niu W, Zang T, Zou Y, Fang S, Smith DK, Bachoo R, Zhang CL. 2013. In vivo reprogramming of astrocytes to neuroblasts in the adult brain. *Nat Cell Biol* 15:1164–1175.
- Nolte C, Matyash M, Pivneva T, Schipke CG, Ohlemeyer C, Hanisch UK, Kirchhoff F, Kettenmann H. 2001. GFAP promoter-controlled EGFP-expressing transgenic mice: A tool to visualize astrocytes and astrogliosis in living brain tissue. *Glia* 33:72–86.
- Pekny M, Nilsson M. 2005. Astrocyte activation and reactive gliosis. *Glia* 50: 427–434.
- Qin S, Niu W, Iqbal N, Smith DK, Zhang CL. 2014. Orphan nuclear receptor TLX regulates astrogenesis by modulating BMP signaling. *Front Neurosci* 8:74.
- Robel S, Berninger B, Gotz M. 2011. The stem cell potential of glia: Lessons from reactive gliosis. *Nat Rev Neurosci* 12:88–104.
- Sakurai K, Osumi N. 2008. The neurogenesis-controlling factor, pax6, inhibits proliferation and promotes maturation in murine astrocytes. *J Neurosci* 28: 4604–4612.
- Su M, Hu H, Lee Y, d’Azzo A, Messing A, Brenner M. 2004. Expression specificity of GFAP transgenes. *Neurochem Res* 29:2075–2093.
- Sun X, Zhang QW, Xu M, Guo JJ, Shen SW, Wang YQ, Sun FY. 2012. New striatal neurons form projections to substantia nigra in adult rat brain after stroke. *Neurobiol Dis* 45:601–609.
- Wang YQ, Cui HR, Yang SZ, Sun HP, Qiu MH, Feng XY, Sun FY. 2009. VEGF enhance cortical newborn neurons and their neurite development in adult rat brain after cerebral ischemia. *Neurochem Int* 55:629–636.
- Wang YQ, Guo X, Qiu MH, Feng XY, Sun FY. 2007. VEGF overexpression enhances striatal neurogenesis in brain of adult rat after a transient middle cerebral artery occlusion. *J Neurosci Res* 85:73–82.
- Yamashita T, Ninomiya M, Hernandez Acosta P, Garcia-Verdugo JM, Sunabori T, Sakaguchi M, Adachi K, Kojima T, Hirota Y, Kawase T, Araki N, Abe K, Okano H, Sawamoto K. 2006. Subventricular zone-derived neuroblasts migrate and differentiate into mature neurons in the post-stroke adult striatum. *J Neurosci* 26:6627–36.
- Zhang QW, Deng XX, Sun X, Xu JX, Sun FY. 2013. Exercise promotes axon regeneration of newborn striatonigral and corticonigral projection neurons in rats after ischemic stroke. *PLoS One* 8:e80139.
- Zhang R, Xue YY, Lu SD, Wang Y, Zhang LM, Huang YL, Signore AP, Chen J, Sun FY. 2006. Bcl-2 enhances neurogenesis and inhibits apoptosis of newborn neurons in adult rat brain following a transient middle cerebral artery occlusion. *Neurobiol Dis* 24:345–356.